J|A|C|S
ARTICLES
Published on Web 08/30/2002

Mechanism of the Photochemical Ligand Substitution Reactions of *fac*-[Re(bpy)(CO)$_3$(PR$_3$)]$^+$ Complexes and the Properties of Their Triplet Ligand-Field Excited States

Kazuhide Koike,*[,†] Nobuaki Okoshi,[†] Hisao Hori,[†] Koji Takeuchi,[†] Osamu Ishitani,*[,‡,||] Hideaki Tsubaki,[‡] Ian P. Clark,[§] Michael W. George,[§] Frank P. A. Johnson,[§] and James J. Turner[§]

Contribution from the National Institute of Advanced Industrial Science and Technology, Onogawa 16-1, Tsukuba 305-8569, Japan, Department of Chemistry, Graduate School of Science and Engineering, Tokyo Institute of Technology, O-okayama 2-12-1, Meguro-ku, Tokyo 152-8551, Japan, CREST, JST (Japan Science and Technology Corporation), 1-8 Honcho, Kawaguchi-shi, Saitama Prefecture 332-0012, Japan, and Department of Chemistry, University of Nottingham, Nottingham NG7 2RD, U.K.

Received September 8, 2001

Abstract: We report herein the mechanism of the photochemical ligand substitution reactions of a series of *fac*-[Re(X$_2$bpy)(CO)$_3$(PR$_3$)]$^+$ complexes (**1**) and the properties of their triplet ligand-field (^{3}LF) excited states. The reason for the photostability of the rhenium complexes [Re(X$_2$bpy)(CO)$_3$(py)]$^+$ (**3**) and [Re(X$_2$bpy)(CO)$_3$Cl] (**4**) was also investigated. Irradiation of an acetonitrile solution of **1** selectively gave the biscarbonyl complexes *cis,trans*-[Re(X$_2$bpy)(CO)$_2$(PR$_3$)(CH$_3$CN)]$^+$ (**2**). Isotope experiments clearly showed that the CO ligand trans to the PR$_3$ ligand was selectively substituted. The photochemical reactions proceeded via a dissociative mechanism from the ^{3}LF excited state. The thermodynamical data for the ^{3}LF excited states of complexes **1** and the corrective nonradiative decay rate constants for the triplet metal-to-ligand charge-transfer (^{3}MLCT) states were obtained from temperature-dependence data for the emission lifetimes and for the quantum yields of the photochemical reactions and the emission. Comparison of **1** with [Re(X$_2$bpy)(CO)$_3$(py)]$^+$ (**3**) and [Re(X$_2$bpy)(CO)$_3$Cl] (**4**) indicated that the ^{3}LF states of some **3**- and **4**-type complexes are probably accessible from the ^{3}MLCT state even at ambient temperature, but these complexes were stable to irradiation at 365 nm. The photostability of **3** and **4**, in contrast to **1**, can be explained by differences in the trans effects of the PR$_3$, py, and Cl$^-$ ligands.

Introduction

The photochemical and photophysical properties of diimine complexes with d^6 metal ions are tremendously interesting from the standpoint of basic science as well as for their practical applications.[1−7] Many of these complexes exhibit the following energetically accessible excited states: charge-transfer (CT), ligand-centered (LC), and ligand-field (LF). An intimate understanding of their energetics and dynamics is important for the design of new useful photochemical devices.

Rhenium diimine complexes of the type *fac*-[Re$^{\mathrm{I}}$(LL)(CO)$_3$L′]$^{n+}$ (n = 0, 1; LL = diimine ligand) have been well studied because they are excellent emitters,[1,8−10] photocatalysts,[6,11−16] and building blocks for supramolecules.[5,17−19] Although a tremendous number of fundamental studies of the photophysics of these rhenium complexes have been carried out over the last two decades, the targets of these studies have been only triplet CT excited states—such as metal-to-ligand

* To whom correspondence should be addressed. E-mail: k-koike@aist.go.jp (K.K.); ishitani@chem.titech.ac.jp (O.I.).
† National Institute of Advanced Industrial Science and Technology.
‡ Tokyo Institute of Technology.
§ University of Nottingham.
|| CREST, JST.

(1) Kalyanasundaram, K. *Photochemistry of polypyridine and porphyrine complexes*; Academic Press Ltd.: London 1992.
(2) Meyer, T. J.; Casper, J. V. *Chem. Rev.* **1985**, *85*, 187−218.
(3) Roundhill, D. M. *Photochemistry and photophysics of metal complexes*; Plenum Press: New York; 1994.
(4) Stufkens, D. J. *Coord. Chem. Rev.* **1990**, *104*, 39−112.
(5) Balzani, V.; Juris, A.; Ventyri, M.; Campagna, S.; Serroni, S. *Chem. Rev.* **1996**, *96*, 759−833.
(6) Kalyanasundaram, K. In *Photosensitization and Photocatalysis using Inorganic and Organometallic Compounds*; Kalyanasundaram, K., Gräzel, M., Eds.; Kluwer Academic Publishers: Dordrecht, The Netherlands, 1993.
(7) Juris, A.; Balzani, V.; Barigeketti, F.; Belser, P.; v. Zelewsky, A. *Coord. Chem. Rev.* **1988**, *84*, 85−277.
(8) Wrighton, M. S.; Morse, D. L. *J. Am. Chem. Soc.* **1974**, *96*, 998.
(9) Casper, J. V.; Meyer, T. J. *J. Phys. Chem.* **1983**, *87*, 952−954.
(10) Kalyanasundaram, K. *J. Chem. Soc., Faraday Trans. 2* **1986**, *82*, 2401.
(11) Hawecker, J.; Lehn, J.-M.; Ziessel, R. *Helv. Chim. Acta* **1986**, *69*, 1990.
(12) (a) Hori, H.; Johnson, F. P. A.; Koike, K.; Ishitani, O.; Ibusuki, T. *J. Photochem. Photobiol., A* **1996**, *96*, 171−174. (b) Hori, H.; Koike, K.; Ishizuka, M.; Takeuchi, K.; Ibusuki, T.; Ishitani, O. *J. Organomet. Chem.* **1997**, *530*, 169−176.
(13) Hori, H.; Johnson, F. P. A.; Koike, K.; Takeuchi, K.; Ibusuki, T.; Ishitani, O. *J. Chem. Soc., Dalton Trans.* **1997**, 1019−1023.
(14) Koike, K.; Hori, H.; Westwell, J. R.; Ishizuka, M.; Takeuchi, K.; Ibusuki, T.; Enjouji, K.; Konno, H.; Sakamoto, K.; Ishitani, O. *Organometallics* **1997**, *16*, 5724−5729.
(15) Pac, C.; Ishii, K.; Yanagida, S. *Chem. Lett.* **1989**, 765.
(16) Tajik, M.; Detellier, C. *J. Chem. Soc., Chem. Commun.* **1987**, 1824.
(17) Slone, R. V.; Benkstein, K. D.; Bélanger, S. J.; Hupp, T.; Guzei, I. A.; Rheingold, A. L. *Coord. Chem. Rev.* **1998**, *171*, 221−243.
(18) Ziessel, R.; Juris, A.; Venturi, M. *Inorg. Chem.* **1998**, *37*, 5061−5069.
(19) Rajendran, T.; Manimaran, B.; Lee, F.-Y.; Lee, G.-H.; Peng, S.-M.; Wang, C. M.; Lu, K.-L. *Inorg. Chem.* **2000**, *39*, 2016−2017.

10.1021/ja017032m CCC: $22.00

(^{3}MLCT),[8,20−25] ligand-to-ligand (^{3}LLCT),[18,26] and σ-to-ligand ($^3\sigma-\pi^*$)[2,27−29] states—and ^{3}LC excited states.[30−32] In contrast, little is known about the LF states of these rhenium diimine complexes. To our knowledge, only one report discusses their triplet ligand-field (^{3}LF) states: this report reveals that the emission lifetimes of *fac*-[Re(LL)(CO)$_3$(CNR)]$^+$ complexes strongly depend on temperature and that the temperature-dependence profiles can be fitted by means of a model based on three thermally accessible excited states: ^{3}MLCT, ^{3}LC, and ^{3}LF.[33] However, this report presents no unambiguous evidence supporting the existence of another excited state, i.e., a ^{3}LF state, other than ^{3}MLCT and ^{3}LC, because *fac*-[Re(LL)(CO)$_3$(CNR)]$^+$ complexes are photostable and because their photochemical ligand substitution reactions, a typical reaction proceeded via the ^{3}LF excited state of d^6 metal complexes, have not been reported so far.

There had been no reports of photochemical ligand substitution reactions of other rhenium diimine tricarbonyl complexes, until we recently reported the first examples as described below,[34] except for complexes with a Re−M (M = metal carbonyl), Re−C, or Re−H bond. The $^3\sigma-\pi^*$ excited states of the complexes are accessible from the ^{3}MLCT states at ambient temperature, and the homolytic dissociation of these bonds proceeds via the $^3\sigma-\pi^*$ excited states.[2,27−29] There are two possible explanations for the photochemical stability of these rhenium complexes: either (1) the energy gap between the lowest excited state and the ^{3}LF state is so large that ^{3}LF is not accessible at ambient temperature or (2) the ^{3}LF state is accessible but not reactive. We have no way to distinguish between these two possibilities. It is surprising that participation of the ^{3}LF excited state has not been considered in most of the studies of rhenium diimine complexes; if it is accessible, the photophysics and photochemistry of these compounds might be affected.[29]

We have found that rhenium polypyridine tricarbonyl complexes with a phosphorus ligand, such as *fac*-[Re(X$_2$bpy)(CO)$_3$(PR$_3$)]$^+$ (**1**; X$_2$bpy = 4,4′-X$_2$-2,2′-bipyridine), are photoactive even at ambient temperature and that excitation of these complexes in acetonitrile solution selectively gives biscarbonyl complexes *cis*,*trans*-[Re(X$_2$bpy)(CO)$_2$(PR$_3$)(CH$_3$CN)]$^+$ (**2**) (eq 1).[34] Because these complexes have no Re−M, Re−C, or Re−H bonds, these reactions are probably the first reported examples of photochemical ligand substitution reactions of rhenium diimine tricarbonyl complexes via their ^{3}LF excited states. Rich information on the "unknown" ^{3}LF excited states of rhenium complexes might be obtained from detailed investigation of the photophysical and photochemical behaviors of **1**.

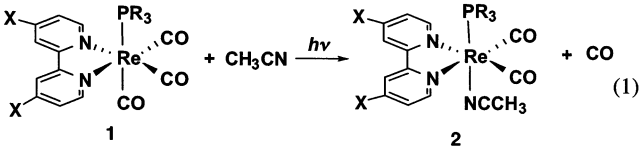

(1)

In this study, we aim to (1) clarify the mechanism of the photochemical ligand substitution reactions of **1**, (2) obtain thermodynamical data on the ^{3}LF states of **1** by using photosubstitution reactions as probes, and (3) investigate why rhenium complexes such as *fac*-[Re(X$_2$bpy)(CO)$_3$Cl] and *fac*-[Re(X$_2$bpy)(CO)$_3$py]$^+$ are photostable.

Experimental Section

Materials. Spectral-grade acetonitrile and CH_2Cl_2 purchased from Kanto Chemical Co., Inc., were dried and distilled over CaH_2 prior to use. ^{13}C-enriched (99.8 atom %) carbon monoxide was purchased from ISOTECH Inc. The synthesis of and spectral data for the rhenium complexes have been reported elsewhere.[12,14]

Measurements. UV−vis absorption spectra were recorded on a Hitachi 330 spectrophotometer or an Otsuka-Denshi Photal-1000 multichannel spectrophotometer with a D_2 (25 W)/I_2 (25 W) mixed lamp. IR spectra were obtained in acetonitrile with a JEOL JIR-6500 FTIR spectrophotometer. Time-resolved infrared (TRIR) absorption spectra were measured at the University of Nottingham by using a third harmonic wave of the Quanta-Ray GCR-12S Nd^{3+}-YAG laser (~7 ns fwhm, ~50 mJ/pulse) as the photolysis source. The changes in IR absorption at particular wavelengths were monitored with CW Mütek MDS4 diode laser elements and a HgCdTe detector (Infrared Associates HCT-100) with "point-to-point" operation. The details of the TRIR apparatus have been described elsewhere.[22,35,36]

Emission Studies. Emission spectra were measured on a Hitachi F-3000 or a JASCO FP-6600 spectrofluorometer. The spectra were corrected for the detector sensitivity by using Rhodamine B, quinine sulfate, and 4-(dimethylamino)-4′-nitrostilbene as standards (Hitachi F-3000) or by using correction data supplied by JASCO (JASCO FP-6600). Emission quantum yields were evaluated with quinine disulfate as a standard. In the emission spectral measurements, the absorbance of all sample solutions was less than 0.1 at the excitation wavelength. The temperatures of the sample solutions in the 1 cm × 1 cm quartz cell were controlled to within 0.1 °C by an EYELA CTP-101 cooling thermo pump. Emission lifetimes were measured with a Horiba NAES-1100 time-correlated single-photon-counting system (the excitation source was a nanosecond H_2 lamp, NFL-111, and the instrument response time was less than 1 ns). Table 1 summarizes the emission data measured at 298 K.

Emission Spectral Fitting. A single-mode Franck−Condon lineshape analysis was used to fit the emission spectra.[37−40] The spectra were calculated with Wavemetrics Igor software on an Apple Macintosh computer, and the parameters were optimized by comparison of calculated and experimental spectra by means of the nonlinear least-

(20) Smothers, W. K.; Wrighton, M. S. *J. Am. Chem. Soc.* **1983**, *105*, 1067.
(21) Stripin, D. R.; Crosby, G. A. *Chem. Phys. Lett.* **1994**, *221*, 426−430.
(22) Ishitani, O.; George, M. W.; Ibusuki, T.; Johnson, F. P. A.; Koike, K.; Nozaki, K.; Pac, C.; Turner, J. J.; Westwell, J. R. *Inorg. Chem.* **1994**, *33*, 4712−4717.
(23) Worl, L. A.; Duesing, R.; Chen, P.; Ciana, L. D.; Meyer, T. J. *J. Chem. Soc., Dalton Trans.* **1991**, 849−858.
(24) Vanhelmont, F. W. M.; Hupp, J. T. *Inorg. Chem.* **2000**, *39*, 1817−1819.
(25) (a) Casper, J. V.; Meyer, T. J. *J. Phys. Chem.* **1983**, *13*, 359. (b) Carlson, D. L.; Murphy, W. R., Jr. *Inorg. Chim. Acta* **1991**, *181*, 61−64.
(26) Schanze, K. S.; MacQueen, D. B.; Perkins, T. A.; Cabana, L. A. *Coord. Chem. Rev.* **1993**, *122*, 63−89.
(27) Rossenaar, B. D.; Kleverlaan, C. J.; M. C. E. Vandeven, M. C. E.; Stufkens, D. J.; Vlček, A., Jr. *Chem.—Eur. J.* **1996**, *2*, 228−237.
(28) Stufkens, D. J. *Comments Inorg. Chem.* **1992**, *13*, 359−385.
(29) Stufkens, D. J.; Vlček, A., Jr. *Coord. Chem. Rev.* **1998**, *177*, 127−179.
(30) Giordano, P. J.; Wrighton, M. S. *J. Am. Chem. Soc.* **1979**, *101*, 2888.
(31) Sacksteder, L.-A.; Zipp, A. P.; Brown, E. A.; Streich, J.; Demas, J. D.; DeGraff, B. A. *Inorg. Chem.* **1990**, *29*, 4335−4340.
(32) Wallace, L.; Rillema, D. P. *Inorg. Chem.* **1993**, *32*, 3836−3843.
(33) Sacksteder, L. A.; Lee, M.; Demas, J. N.; Degraff, B. A. *J. Am. Chem. Soc.* **1993**, *115*, 8230−8238.
(34) Koike, K.; Tanabe, J.; Toyama, S.; Tsubaki, H.; Sakamoto, K.; Westwell, J. R.; Johnson, F. P. A.; Hori, H.; Saitoh, H.; Ishitani, O. *Inorg. Chem.* **2000**, *39*, 2777.
(35) Dixon, A. J.; Healy, M. A.; Hodges, P. M.; Moore, B. D.; Poliakoff, M.; Simpson, M. B.; Turner, J. J.; West, M. A. *J. Chem. Soc., Faraday Trans. 2* **1986**, *82*, 2083.
(36) George, M. W.; Poliakoff, M.; Turner, J. J. *Analyst (London)* **1994**, *119*, 551.
(37) Worl, L. A.; Duesing, R.; Chen, P.; Della Ciana, L.; Meyer, T. J. *J. Chem. Soc., Dalton Trans.* **1991**, 849.
(38) Caspar, J. V.; Kober, E. M.; Sullivan, B. P.; Meyer, T. J. *J. Am. Chem. Soc.* **1982**, *104*, 630.
(39) Wang, Y.; Schanze, K. S. *Inorg. Chem.* **1994**, *33*, 1354.
(40) Walters, K. A.; Schanze, K. S. *Spectrum* **1998**, *11*, 1.

Table 1. Emission Data for the Rhenium Bipyridine Tricarbonyl Complexes and Quantum Yields of the Photochemical Ligand Substitution Reactions (Φ_r) of **1** in CH_3CN at 298 K

	$[Re(X_2bpy)(CO)_3(PR_3)]^+$		λ_e	τ_e		
	X	PR_3	(nm)	(ns)	Φ_e	Φ_r
1a	H	$P(OEt)_3$	542	1034	0.155	0.089
1b	CH_3	$P(OEt)_3$	533	936	0.175	0.16
1c	CF_3	$P(OEt)_3$	623	162	0.031	0.0003
1d	H	$P(n\text{-}Bu)_3$	561	621	0.091	0.095
1e	H	PEt_3	561	654	0.153	0.15
1f	H	PPh_3	540	416	0.097	0.55
1g	H	$P(OMe)Ph_2$	542	644	0.127	0.25
1h	H	$P(O\text{-}i\text{-}Pr)_3$	543	952	0.247	0.099
1i	H	$P(OMe)_3$	543	1076	0.216	0.118

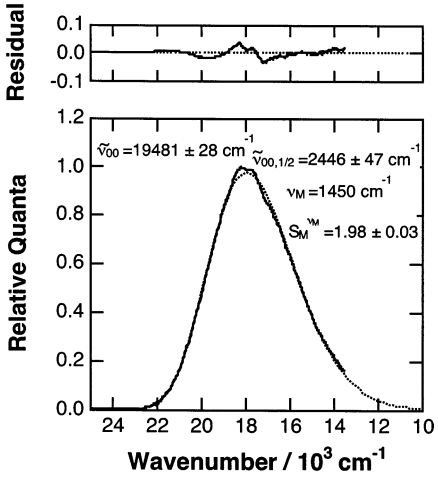

Figure 1. Corrected emission spectrum of **1a**. The solid line was obtained from the experimental data, and the dotted line is a spectrum calculated by means of a single-mode Franck−Condon line-shape analysis.

squares method. Equation 2 was used for the calculated spectra. $I(\tilde{\nu})$ is

$$I(\tilde{\nu}) = \sum_{\nu_m=0}^{5}\left\{\left(\frac{\tilde{\nu}_{00}-\nu_m h\varpi_m}{\tilde{\nu}_{00}}\right)^3 \frac{S_m^{\nu_m}}{\nu_m}\right\}\exp\left[-4\ln 2\left(\frac{\tilde{\nu}_{00}-\nu_m h\varpi_m}{\Delta\tilde{\nu}_{00,1/2}}\right)^2\right] \quad (2)$$

the relative emission intensity at frequency $\tilde{\nu}$, $\tilde{\nu}_{00}$ is the 0−0 emission energy, $h\varpi_m$ is the average of medium-frequency acceptor modes that are coupled to the electronic transition, $S_m^{\nu_m}$ is the electron-vibration coupling constant (Huang−Rhys factor), and $\Delta\tilde{\nu}_{00,1/2}$ is the half-width of the 0−0 vibronic band; the sum is taken over the quantum number of the average medium-frequency vibrational mode (ν_m). A value for $h\varpi_m$ of 1450 cm^{-1} was used in all of the fits.[37] As a typical example, the fit for **1a** is shown in Figure 1. Similarly good fits were obtained for other complexes. The 0−0 band energy gaps between ^{3}MLCT and the ground state ($E_{00}(^3\text{MLCT})$) were obtained from the calculated spectra.

Photolysis. An Ushio 350 W high-pressure Hg lamp was used as a light source, and the 365 nm monochromatic light was introduced into a Pyrex vessel with a 10-cm path length solution filter of $CuSO_4$ (0.46 M) and a Shimazu M250 monochromator. The irradiation light intensity, 4.24×10^{15} photons s^{-1}, was calculated with a $K_3Fe(C_2O_4)_3$ chemical actinometer. A gentle stream of argon was bubbled into an acetonitrile solution of **1** (0.12 mM) for 15 min, and the solution was then photolyzed. The temperature of the solution was controlled by means of the cooling thermo pump described above. The photochemical reactions were monitored with the Otsuka-Denshi Photal-1000 multichannel spectrophotometer. In all reactions except for that of **1c**, one set of isosbestic points was observed until the starting complexes completely disappeared, and therefore, the photochemical reactions proceeded quantitatively. On the basis of these observations, we determined the molecular absorption coefficients of products **2** (ϵ_2) from the final spectra of the irradiated solutions, as shown in Table 2. We have isolated **2a** and **2f**,[34] and their molecular absorption coefficients are in good agreement with the ϵ_2 values in Table 2. Using these data and eq 3, we calculated the concentrations of product **2** and starting

Table 2. UV−Vis Absorption Spectral Data for $[Re(X_2bpy)(CO)_2(PR_3)(CH_3CN)]^+$ (**2**) in CH_3CN at 298 K

	2		λ_{max}	ϵ_2
	X	PR_3	(nm)	(M^{-1} cm^{-1})
a	H	$P(OEt)_3$	375	3900
b	CH_3	$P(OEt)_3$	375	4000
c[a]	CF_3	$P(OEt)_3$		
d	H	$P(n\text{-}Bu)_3$	427	3600
e	H	PEt_3	422	3600
f	H	PPh_3	405	3600
g	H	$P(OMe)Ph_2$	392	3100
h	H	$P(O\text{-}i\text{-}Pr)_3$	382	3100
i	H	$P(OMe)_3$	374	2500

[a] See the text.

$$[\mathbf{2}] = [\mathbf{1}]_0 - [\mathbf{1}] = \frac{A(\lambda) - A_0(\lambda)}{(\epsilon_2(\lambda) - \epsilon_1(\lambda))d} \quad (3)$$

material **1** after irradiation. d is the path length (1 cm), $A(\lambda)$ is the absorbance at the monitoring wavelength, $A_0(\lambda)$ is the initial absorbance at λ, and ϵ_1 and ϵ_2[12b] are the molecular absorption coefficients at λ of **1** and **2**, respectively. We also observed a set of isosbestic points in the first stage of the photochemical reaction of **1c.** However, the photoreactivity of **1c** was low, and some byproducts were produced upon prolonged irradiation. Therefore, we determined the concentration of **1c** using HPLC.[41]

^{13}C NMR Study of the Photochemical Reaction of 1a. A $CDCl_3$ solution (1 mL) containing **1a** (16.5 mM) was degassed by means of the freeze−pump−thaw method and transferred into a 5 mm ∅ NMR tube (total volume ~4 mL). After 550 mmHg of ^{13}CO gas (^{13}C content 99.8 atom %) was introduced through a vacuum line, the NMR tube was shaken for several minutes, and the tube was then sealed with a torch. The solution was irradiated with 365 nm light in the apparatus described above. The ^{13}C NMR spectra of the solution at various times during irradiation were measured on a JEOL Lambda 500 system (125 MHz) by using $CDCl_3$ as an internal standard. Integration of the peaks obtained by the NOE complete ^{1}H-decoupling method (EXMOD: nne) was used for determining the relative concentrations of the ^{13}CO ligands; the methylene carbons of the $P(OEt)_3$ ligand were used as an internal standard.

Results and Discussion

Mechanism of the Photochemical Ligand Substitution Reactions. As a typical example of the spectra observed for the photochemical ligand substitution reactions, the in situ UV−vis absorption spectra obtained during irradiation of an acetonitrile solution containing **1a** are shown in Figure 2. A set of isosbestic points was observed, and the final spectrum was identical to that of isolated **2a**, which indicates that the reaction proceeded quantitatively and that product **2a** was photochemically stable. Irradiation of acetonitrile solutions containing other *fac*-$[Re(X_2bpy)(CO)_3(PR_2R')]^+$-type complexes (**1**; X = H, CH_3, CF_3; R = R′ = Ph, Et, *n*-Bu, O-*i*-Pr, OPh, OMe; R = Ph, and R′ = OEt) caused similar ligand substitution reactions; i.e., *cis,trans*-$[Re(X_2bpy)(CO)_2(PR_2R')(CH_3CN)]^+$ complexes were

(41) Hori, H.; Koike, K.; Ishizuka, M.; Westwell, J. R.; Takeuchi, K.; Ibusuki, T.; Ishitani, O. *Chromatographia* **1996**, *43*, 251.

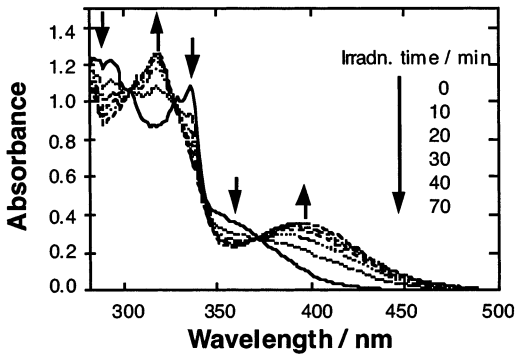

Figure 2. In situ UV−vis absorption spectral changes in a CH_3CN solution containing **1a** (0.12 mM) under an Ar atmosphere during irradiation at 365 nm.

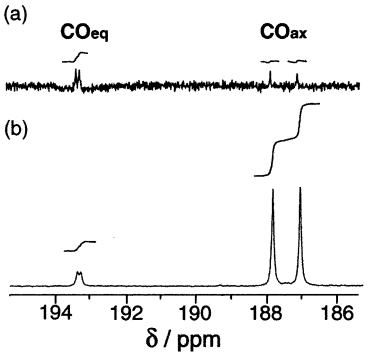

Figure 3. ^{13}C NMR spectra of **1a** in a $CDCl_3$ solution under a ^{13}CO atmosphere: (a) before irradiation (10000× accumulation) and (b) after 60 min of irradiation (18000× accumulation).

formed quantitatively. The quantum yields of the photochemical ligand substitution reactions at 25 °C (Φ_r) are shown in Table 1. In all cases, neither *cis,cis*-[Re(X_2bpy)(CO)$_2$(PR$_2$R′)(CH_3CN)]$^+$ nor [Re(X_2bpy)(CO)$_3$(CH_3CN)]$^+$ was observed, which indicates that acetonitrile was selectively introduced into a position trans to the phosphorus ligand.

There are two possible mechanisms for this selectivity: in one mechanism, only the axial CO ligand, which is trans to the phosphorus ligand, is photolabile (eq 4), and in the other mechanism, the dissociation of the equatorial CO ligands is accompanied by a shift of the axial CO to the open equatorial position and subsequent occupation of the axial position by the acetonitrile molecule (eq 5).

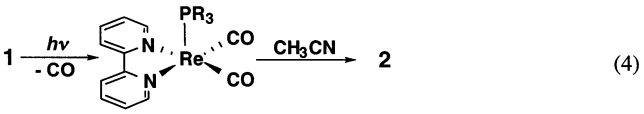

(4)

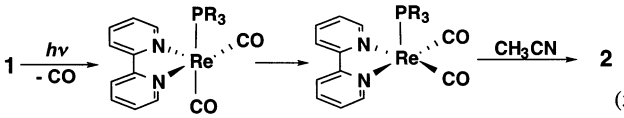

(5)

We employed ^{13}C NMR spectroscopy to determine which mechanism was operating. Figure 3a shows the ^{13}C peaks in the carbonyl region of a ^{13}CO-saturated $CDCl_3$ solution containing **1a** before irradiation. We attributed the two sets of peaks, at 193.2 and 193.1 ppm and at 187.8 and 187.1 ppm, to one axial and two equivalent equatorial CO ligands, respectively, on the basis of their peak areas and the coupling constants with

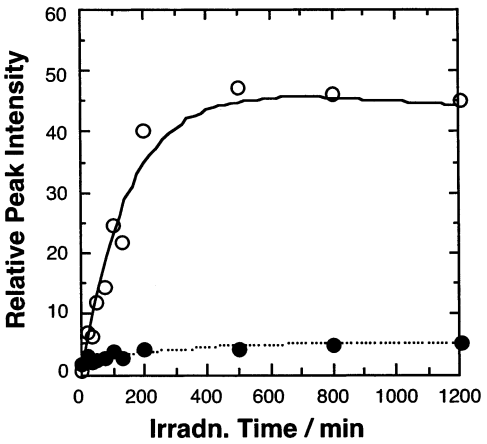

Figure 4. Intensity change in the ^{13}C NMR signals for the axial (○) and the equatorial (●) CO ligands of **1a** in a $CDCl_3$ solution during irradiation (365 nm) under a ^{13}CO atmosphere. The methylene carbon signal of the P(OEt)$_3$ ligand was used as an internal standard.

the phosphorus atom of the ligand. Irradiation of the solution caused a tremendous increase in the axial ^{13}CO peaks but almost no change in the equatorial ^{13}CO peaks, as shown in Figure 3b. Figure 4 shows the changes in the ^{13}C peak intensities of the CO ligands at various times during irradiation. Even after a photochemical stationary state was almost reached (=500 min), we observed only a small increase in the peak areas of the equatorial ^{13}CO ligands. If the photochemical ligand substitution reaction with ^{13}CO proceeded by means of a shift of the axial CO to the equatorial position, the ^{13}C content at the equatorial CO ligand should increase at least after the photochemical stationary state is reached (eq 6). These results clearly indicate that the operative mechanism is that shown in eq 4, i.e., the site-selective substitution of the axial CO ligand.

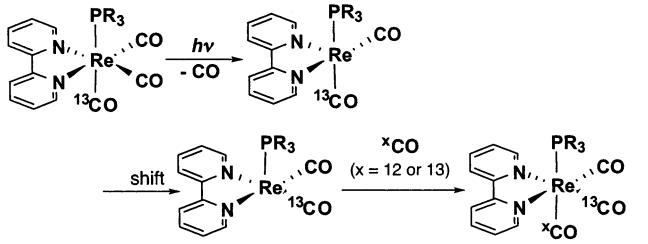

(6)

Another mechanistic question is whether the photochemical ligand substitution reactions proceed via a dissociative or an associative mechanism. Irradiation of a CH_2Cl_2 solution of **1a** in the presence of reagents L (240 mM) having different nucleophilicities—e.g., CH_3CN, pyridine, and P(OEt)$_3$—gave *cis,trans*-[Re(bpy)(CO)$_2${P(OEt)$_3$}(L)]$^+$ quantitatively, and neither the type nor the concentration of the added reagent affected the quantum yields of the formation of these products. Consequently, the photochemical ligand substitution reaction of **1a**, and presumably also that of **1b**−**i**, probably proceeds via the dissociative mechanism shown in eqs 7 and 8.

$$[Re(bpy)(CO)_3(PR_3)]^+ \xrightarrow{h\nu} [Re(bpy)(CO)_2(PR_3)]^+ + CO \quad (7)$$

$$[Re(bpy)(CO)_2(PR_3)]^+ + L \rightarrow [Re(bpy)(CO)_2(PR_3)(L)]^+ \quad (8)$$

Reactive Excited State. We used TRIR spectroscopy to obtain information about the excited state from which the

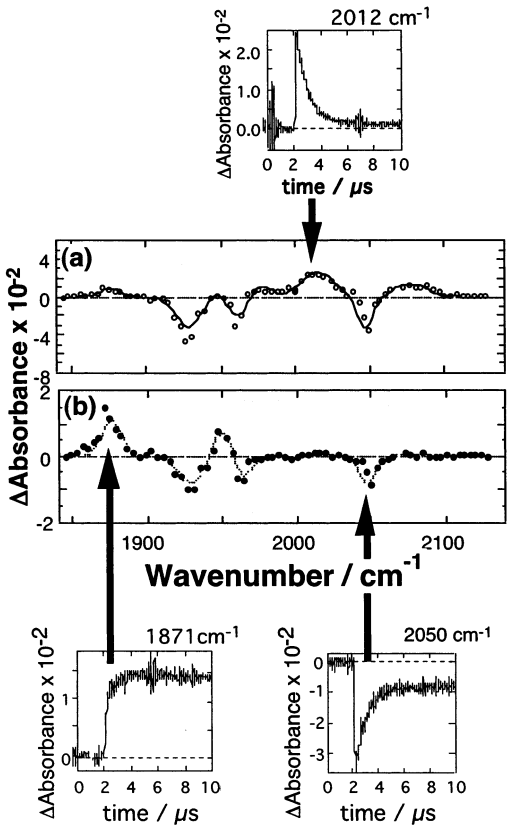

Figure 5. Transient IR spectra of **1a** in a degassed CH_3CN solution taken at 50 ns (a) and 5 μs (b) after 355 nm laser excitation. The three insets represent the typical decay traces for different IR bands.

photochemical ligand substitution reaction occurs. Figure 5 shows the ν(CO) region in the TRIR spectra after laser excitation of **1a** in an Ar-saturated acetonitrile solution. Immediately after the laser flash, we observed three negative peaks (at 1928, 1962, and 2047 cm^{-1}), which indicate a decrease in the concentration of the ground state of **1a**, and three positive peaks at higher wavenumbers attributable to the ^{3}MLCT excited state (~1970, 2017, and ~2070 cm^{-1}) (Figure 5a).[42] Figure 5b shows the spectrum 5 μs after the laser excitation: the ^{3}MLCT state has disappeared, a set of new peaks at 1876 and 1951 cm^{-1}, which coincide with the peaks for product **2a**, has increased, and there is partial recovery of the peaks of the ground state. Figure 5 also illustrates the temporal behavior of the three peaks attributable to the ^{3}MLCT state (2012 cm^{-1}), the ground state (2050 cm^{-1}) of **1a**, and the ground state of **2a** (1871 cm^{-1}). The good agreement among the first-order rate constants obtained from these data (1.2×10^{-6}, 1.1×10^{-6}, and 1.6×10^{-6} s^{-1}, respectively) clearly indicates that the photochemical ligand substitution reaction of **1a** to form **2a** proceeded via either the ^{3}MLCT state of **1a** or another excited state (RS) that was thermally accessible from the ^{3}MLCT state.

Studies of the temperature dependence of the reactions and the emissions gave additional information. The quantum yields of the photochemical reactions of **1a**−**i** (Φ_r) increased at higher temperatures. A typical example, the case of **1a**, is shown in

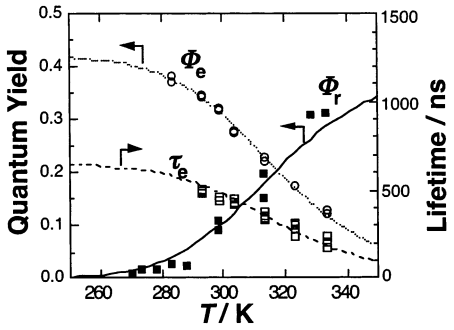

Figure 6. Temperature dependence of the emission yield (Φ_e) and lifetime (τ_e), and the quantum yield of the photochemical ligand substitution reaction (Φ_r) of **1a** in a degassed CH_3CN solution.

Scheme 1. Jablonski Diagram Describing the Mechanism of the Photoinduced Ligand Substitution Reaction of **1**

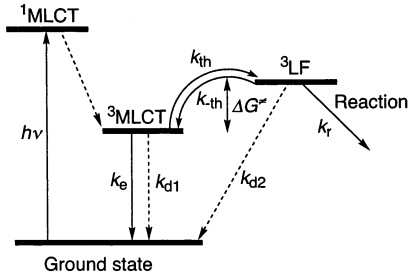

Figure 6. We also found that the lifetime (τ_e) and the quantum yield (Φ_e) of the emission that occurred from the ^{3}MLCT excited state[5,6] depended strongly on the temperature of the solution (Figure 6). We should point out that, unlike Φ_r, both Φ_e and τ_e decreased at higher temperature. These results strongly suggest that the photochemical ligand substitution reaction occurred via an excited state (RS) thermally accessible from the ^{3}MLCT state. Photochemical ligand substitution reactions of many transition-metal diimine complexes are known to proceed via the ^{3}LF excited state that is thermally accessible from the ^{3}MLCT state, especially when the photosubstitution occurs by a dissociative mechanism.[45] We can interpret all of the experimental results for the photosubstitutions of **1a**−**i** with the energy diagram shown in Scheme 1. However, more-detailed thermodynamic studies are required before we can definitively assign the RS state to ^{3}LF because, as discussed below, we lack information about the ^{3}LF states of the rhenium diimine complexes.

On the basis of the energy diagram in Scheme 1, the temperature dependence of the quantum yields of the emission and the reaction (Φ_e and Φ_r) and the emission lifetime (τ_e) can be described by eqs 9−13.[43]

$$\Phi_e = k_e/(k_e + k_{d1} + k(T)) \quad (9)$$

$$\Phi_r = k_r'/(k_e + k_{d1} + k(T)) \quad (10)$$

$$\tau_e = 1/(k_e + k_{d1} + k(T)) \quad (11)$$

$$k_r' = \Phi_r/\tau_e = \{k_r/(k_r + k_{d2})\}k(T) \quad (12)$$

$$k(T) = \{k_{th}(k_r + k_{d2})\}/(k_{-th} + k_r + k_{d2}) \quad (13)$$

(42) Similar frequency shifts of the ν(CO) peaks have been reported for the ^{3}MLCT states of other rhenium bipyridine carbonyl complexes, such as $Re(bpy)(CO)_3Cl$[44] and $[Re(bpy)(CO)_2\{P(OEt)_3\}_2]^+$.[22] These shifts can be explained as follows: the lower electron density on the rhenium metal in the ^{3}MLCT state causes a decrease in π-back-donation to the π^* orbitals of the carbonyl ligands, which weakens the CO bonds.

(43) Thorburn, I. S.; Rettig, S. J.; James, B. R. *Inorg. Chem.* **1986**, *25*, 227−234.

(44) George, M. W.; Johnson, F. P. A.; Westwell, J. R.; Hodges, P. M.; Turner, J. J. *J. Chem. Soc., Dalton Trans.* **1993**, 2977.

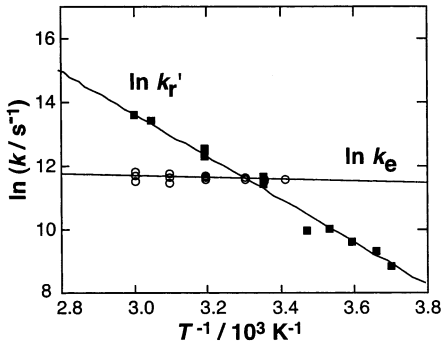

Figure 7. Arrhenius plots of the radiative decay rate (k_e) and the reaction rate of the photochemical ligand substitution reaction (k_r') of **1a** in a degassed CH_3CN solution.

Constants k_{d1} and k_{d2} are the nonradiative decay rate constants for the ^{3}MLCT and ^{3}LF states, respectively. The rate constants k_{th} and k_{-th} are the forward and backward internal conversion rates between the ^{3}MLCT state and the RS state, and depend on the thermal activation between these two states. The temperature-dependent component can be summarized in a single term, $k(T)$ (eq 13). We can analyze the temperature dependence of the observed reaction rate k_r' by considering the two limiting cases (1) $k_{-th} \ll k_r + k_{d2}$ and (2) $k_{-th} \gg k_r + k_{d2}$.

In case 1, the temperature-dependent term is the forward thermal activation rate k_{th}; i.e., $k(T) = k_{th}$. Consequently, k_r' can be described by eq 14, where ΔE_r is the activation energy and k_{th}^0 is the preexponential factor for the forward internal conversion process.

$$k_r' = \{k_r/(k_r + k_{d2})\}k_{th}^0 \exp(-\Delta E_r/RT) \qquad (14)$$

In case 2, where thermal equilibrium is achieved, $k(T) = (k_{th}/k_{-th})(k_r + k_{d2})$ and, consequently, $k_r' = (k_{th}/k_{-th})k_r$. In this equilibrium, k_{th}/k_{-th} should have an Arrhenius-type temperature dependence and k_r' can be described by eq 14′, which is similar to the equation used for case 1 except that the preexponential factor k_r^0 becomes $(k_{th}^0/k_{-th}^0)k_r$.

$$k_r' = (k_{th}^0/k_{-th}^0)k_r \exp(-\Delta E_r/RT) \qquad (14')$$

Consequently, the temperature dependence of the observed reaction rate k_r should be represented by eq 15 in both cases. $k_r^0 = \{k_r/(k_r + k_{d2})\}k_{th}^0$ (case 1), or $k_r^0 = (k_{th}^0/k_{-th}^0)k_r$ (case 2).

$$k_r' = k_r^0 \exp(-\Delta E_r/RT) \qquad (15)$$

As a typical example, the results for k_r' of **1a** are shown in Figure 7. The emission rate constant k_e, which can be calculated as Φ_e/τ_e, is also plotted. The Arrhenius plots for both k_r' and k_e show good linear relationships, as do the plots for the other complexes. However, the activation energies for the ligand substitution reactions were far different from those for the emissions. In the case of **1a**, the values of ΔE_r and k_r^0 were 4620 ± 314 cm^{-1} and (4.11 ± 14.0) × 10^{14} s^{-1}, respectively, which represent the values for the thermal activation of ^{3}MLCT to RS. However, k_e was almost independent of the temperature in the range from 273 to 333 K (1.5 × 10^5 s^{-1}). This result is reasonable because the emissive ^{3}MLCT is the lowest excited state in this temperature range.

The thermodynamical data on the photochemical ligand substitution reactions of **1a**−**i**, which were calculated from the temperature-dependence results for k_r' and eq 15, are summarized in Table 3, along with the 0−0 band energy gaps between the ground state and the ^{3}MLCT states, $E_{00}(^3\text{MLCT})$. Complexes **1a**−**i** all show similar and positive $\Delta S^{\ddagger}$ values, which suggests that their transition states are similar and that the ligand substitution reactions proceed via the same dissociative mechanism. The sum of $E_{00}(^3\text{MLCT})$ and the activation free energy change, i.e., $(E_{00} + \Delta G^{\ddagger})_{298}$, is the energy gap between the transition state of the ligand substitution reactions and the ground state at 298 K, and because of the structural similarities among **1a**−**i,** it is reasonable that this value closely approximates the energy of the RS state or the thermal activation barrier to the RS state. The introduction of strongly electron-withdrawing CF_3 groups into the 4 and 4′ positions of the bipyridine ligand (**1c**) greatly decreased the ^{3}MLCT energy level of this complex (by nearly 2200 cm^{-1}) compared to that of bpy complex **1a**. In contrast, the ^{3}MLCT energy level of **1b,** which bears electron-donating CH_3 groups in the bpy ligand, was 170 cm^{-1} higher than that of **1a**. However, the differences in the activated state energies for these three complexes were less than 1200 cm^{-1}. Therefore, the reactive state energies, unlike the ^{3}MLCT energies, are not sensitive to the substituents on the bipyridine ligand. However, the electronic properties of the phosphorus ligands affected both the reactive state energies and the ^{3}MLCT energies similarly. These results unambiguously support the hypothesis that the RS state is ^{3}LF.

There are three possible relaxation pathways through the ^{3}LF state: (1) a photodissociation that gives reaction products, (2) a photodissociation and successive recombination, and (3) a direct nonradiative decay to the ground state. An apparent nonradiative decay rate from ^{3}LF (k_{d2}' in eq 16) that occurs by pathway 2 or pathway 3 or both can be described by eq 17, on the basis of a treatment similar to that of k_r' in eq 15. Consequently, eqs 9−11 can be rewritten as eqs 9′−11′. In eqs 16 and 17, $k_{d2}^0 = \{k_{d2}/(k_r+k_{d2})\}k_{th}^0$ (case 1) or $k_{d2}^0 = (k_{th}^0/k_{-th}^0)k_{d2}$ (case 2).

$$k_{d2}' = \{k_{d2}/(k_r + k_{d2})\}k(T) \qquad (16)$$

$$k_{d2}' = k_{d2}^0 \exp(-\Delta E_r/RT) \qquad (17)$$

$$\Phi_e = k_e/\{k_e + k_{d1} + (k_r^0 + k_{d2}^0)\exp(-\Delta E_r/RT)\} \qquad (9')$$

$$\Phi_r = k_r^0 \exp(-\Delta E_r/RT)/\{k_e + k_{d1} + (k_r^0 + k_{d2}^0)\exp(-\Delta E_r/RT)\} \qquad (10')$$

$$\tau_e = 1/\{k_e + k_{d1} + (k_r^0 + k_{d2}^0)\exp(-\Delta E_r/RT)\} \qquad (11')$$

The temperature dependence of Φ_e, Φ_r, and τ_e was well simulated by using eqs 9′−11′ and the obtained values of k_e, k_r^0, and ΔE_r but could not be simulated if the temperature-dependent nonradiative decay pathways 2 and 3 were excluded.

The evaluated rate constants k_{d1} and k_{d2}^0 were 7.3 × 10^5 and 8 × 10^{14} s^{-1} for **1a**. Comparison of k_r^0 with k_{d2}^0 shows that nonradiative decay from the ^{3}LF state competed with the ligand substitution process. Both the nonradiative decay and the reaction pathways from the ^{3}LF state were extremely fast (with rate constants >10^{14} s^{-1}); this suggests that the ^{3}LF excited states of the complexes have repulsive potential curves, as in case 1, and that the temperature-dependent nonradiative decay

Table 3. Thermodynamical Data for the Photochemical Ligand Substitution Reactions of $[Re(X_2bpy)(CO)_3(PR_3)]^+$ (**1**) in CH_3CN

1			$E_{00}(^3MLCT)^a$	k_{d1}			$\Delta G^{\ddagger}_{298}{}^b$	$(E_{00}+\Delta G^{\ddagger})_{298}$
	X	PR_3	(cm^{-1})	($10^5\ s^{-1}$)	$\Delta H^{\ddagger}$ (kJ mol^{-1})	$\Delta S^{\ddagger}$ (J $mol^{-1}\ K^{-1}$)	(cm^{-1})	(cm^{-1})
a	H	$P(OEt)_3$	19470 ± 55	6.9	52.8 ± 3.8	26.5 ± 12.3	3810 ± 590	23280 ± 650
b	CH_3	$P(OEt)_3$	19637 ± 50	4.1	47.2 ± 0.5	13.2 ± 1.6	3650 ± 80	23290 ± 130
c	CF_3	$P(OEt)_3$	17272 ± 49	60	65.6 ± 0.9	29.3 ± 2.8	4820 ± 140	22090 ± 190
d	H	$P(n\text{-}Bu)_3$	18672 ± 50	11	48.7 ± 5.2	26.0 ± 17.0	3480 ± 830	22150 ± 880
e	H	PEt_3	18649 ± 51	11	44.3 ± 3.9	14.0 ± 12.5	3390 ± 610	22030 ± 660
f	H	PPh_3	19000 ± 31	8.5	46.1 ± 10.3	27.5 ± 34.6	3230 ± 1650	22230 ± 1680
g	H	$P(OMe)Ph_2$	19553 ± 46	9.7	42.4 ± 2.8	13.3 ± 9.1	3240 ± 440	22790 ± 490
h	H	$P(O\text{-}i\text{-}Pr)_3$	19239 ± 52	7.9	49.8 ± 4.8	24.6 ± 15.6	3610 ± 760	22840 ± 810
i	H	$P(OMe)_3$	19678 ± 43	6.2	50.4 ± 4.8	20.9 ± 15.7	3740 ± 760	23420 ± 800

[a] 0−0 band energy gap between the ^{3}MLCT and the ground states. [b] Free activation energy change at 298 K.

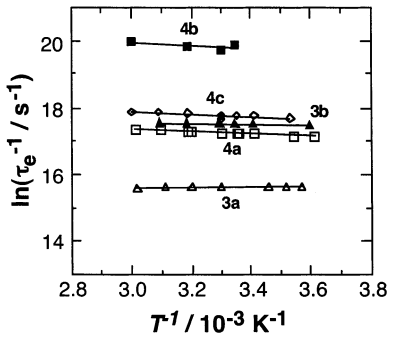

Figure 8. $\ln(\tau_e^{-1})$ vs T^{-1} for the series of *fac*-$[Re(X_2bpy)(CO)_3Y]^{n+}$ complexes (Y = py, Cl^-) in CH_3CN.

Table 4. Photophysical and Thermodynamical Data for $[Re(X_2bpy)(CO)_3Y]^{n+}$ Complexes in CH_3CN

complex	X	Y	n	k_{d1} ($10^5\ s^{-1}$)	$E_{00}(^3MLCT)^a$ (cm^{-1})	$\Delta G^{\ddagger}_{298}{}^b$ (cm^{-1})
1c	CF_3	$P(OEt)_3$	1	60	17270 ± 50	4820 ± 140
3a	H	py	1	40	17490 ± 15	−36 ± 15
3b	CF_3	py	1	400	15090 ± 15	84 ± 8
4a	H	Cl^-	0	320	15660 ± 30	250 ± 21
4b	CF_3	Cl^-	0	4100	13680 ± 20	252 ± 94
4c	OMe	Cl^-	0	520	16320 ± 1	252 ± 40

[a] 0−0 band energy gaps between the ^{3}MLCT and the ground states. [b] Free activation energy change at 298 K.

processes proceed via CO ligand dissociation and successive recombination of the produced species, i.e., $[Re(X_2bpy)(CO)_2(PR_3)]^+$ and CO, in a solvent cage.

Photostabilities of Chloride and Pyridine Complexes. In this paper, we have shown that the ^{3}LF excited states of rhenium diimine tricarbonyl complexes with a phosphorus ligand are thermally accessible from the ^{3}MLCT states at ambient temperature. To investigate whether the same is true for other rhenium complexes, we checked the photostabilities of $[Re(X_2bpy)(CO)_3(py)]^+$ (**3**; py = pyridine; X = H, CF_3) and $[Re(X_2bpy)(CO)_3Cl]$ (**4**; X = H, CF_3, OMe), which were confirmed to be stable to irradiation at 365 nm, in accordance with "common knowledge". Figure 8 illustrates Arrhenius plots for the emission lifetimes of **3** and **4**. Their temperature dependencies were much smaller than those for **1a**−**i** between 10 and 60 °C. The activation free energy changes ($\Delta G^{\ddagger}_{298}$) obtained from these data together with k_{d1} and $E_{00}(^3MLCT)$ are summarized in Table 4.

The photostabilities of the rhenium complexes have been explained, without clear evidence, by large band gaps between the ^{3}LF and ^{3}MLCT states.[29,45] However, for at least some

(45) Vlček, A., Jr. *Coord. Chem. Rev.* **1998**, *177*, 219.

Scheme 2. Energy vs Re−CO Distance for Rhenium Complexes, Illustrating the Three Lowest-Lying Electronic States: (a) $[Re\{(CF_3)_2bpy\}(CO)_3\{P(OEt)_3\}]^+$ (1c), (b) $[Re(bpy)(CO)_3(py)]^+$ (3a) and $[Re\{(CH_3O)_2bpy\}(CO)_3Cl]$ (4c) for the Case of a Nonreactive ^{3}LF State, and (c) 3a and 4c for the Case of a Large Activation Energy from the ^{3}MLCT to ^{3}LF States

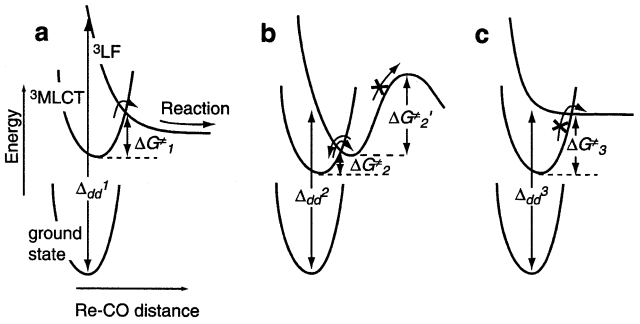

complexes, the explanation is not so simple, for the following reasons. The energy level of the ^{3}MLCT state of **3a**, i.e., $E_{00}(^3MLCT)$ of $[Re(bpy)(CO)_3(py)]^+$, is 220 cm^{-1} higher than that of **1c** (Tables 3 and 4). Moreover, the d−d energy splitting of **3a** ($\Delta_{dd}{}^2$ or $\Delta_{dd}{}^3$ in Scheme 2) should be smaller than that of **1c** ($\Delta_{dd}{}^1$) because of the weaker ligand-field strengths of py and bpy compared to $P(OEt)_3$ and $(CF_3)_2bpy$, respectively. Similar reasoning can be applied to the Cl^- complex $[Re\{(CH_3O)_2bpy\}(CO)_3Cl]$ (**4c**). Thus, **3a** and **4c** are photostable even though their ^{3}MLCT energies are higher and their ^{3}LF energies are lower than those of **1c**, respectively. This can be explained in two ways.

Scheme 2a illustrates the potential energies of the low-lying electronic states (the ground state, the ^{3}MLCT state, and the ^{3}LF state) of **1c** vs the bond distance between the rhenium metal center and the axial-CO carbon atom. The ^{3}LF state exhibits a repulsive potential energy curve (PEC) and is accessible from the ^{3}MLCT state by thermal activation ($\Delta G^{\ddagger}_1$).

The PECs of **3a** and **4c** can be illustrated in two ways (Scheme 2b,c):

(1) The PEC of the ^{3}LF state crosses the PEC of the ^{3}MLCT state at a lower activation energy than that of **1c** ($\Delta G^{\ddagger}_2 < \Delta G^{\ddagger}_1$), but there is an extra potential barrier along the Re−CO dissociation coordinate, a barrier that has a rather high activation energy ($\Delta G^{\ddagger}_2{}'$) because of the trans effect (Scheme 2b). The Re−C bond of the CO ligand trans to the phosphorus ligand is much weaker than the Re−C bonds of the chloride complex and the pyridine complex because of the stronger π-acidity of PR_3 compared to the π-base Cl^- and the weaker π-acid py.[46] When the complexes are excited to the ^{3}LF states and the bonds between the central rhenium and the ligands are weakened, the weakest bonds, i.e., the Re−CO (axial) bonds of **1a**−**i**, are

broken, whereas the Re−CO bonds in **3** and **4** might not be weak enough to be broken. (2) The PEC of the ^{3}LF state crosses the PEC of the ^{3}MLCT state at an energy higher than that of **1c** because the potential well of the ^{3}LF state is much shallower than that of **1c** (Scheme 2c). In this case, the activation energies ($\Delta G^{\ddagger}_3$) are potentially higher than the activation energy of **1c** ($\Delta G^{\ddagger}_1$), even if they have smaller d−d energy splittings ($\Delta_{dd}{}^3 < \Delta_{dd}{}^1$).

Because compounds **1c**, **3a,** and **4c** have similar molecular structures, it is not unlikely that the curvatures of their ^{3}LF excited-state potential surfaces dramatically change despite having the same CO leaving group in the reaction. The first explanation seems more favorable and is also useful for explaining the positional selectivity of the photochemical loss of CO in **1a**−**i** as described above: the PR$_3$ ligand has a much stronger trans effect than the X$_2$bpy ligand.

We cannot clearly discriminate between the mechanisms for the photostabilities of other Cl$^-$ and py complexes (Table 4) at this point, because the energy levels of their ^{3}LF states and their ^{3}MLCT states are lower than those of **1a**−**i** and because we cannot obtain quantitative data for the ^{3}LF states of the Cl$^-$ and py complexes. However, we can assume that many of the Cl$^-$ and py complexes might be stable even when excited to the ^{3}LF state for the reasons delineated in this section.

Energy Gap Law. Nonradiative decay processes for various types of transition-metal complexes have been investigated by using the energy gap law.[25] Casper and Meyer have reported that there is a good linear relationship between the energy gap and the ln "k_d" values, which are "nonradiative decay rate constants from ^{3}MLCT of [Re(X$_2$bpy)(CO)$_3$Y]$^{n+}$" calculated from only emission quantum yields, lifetimes, and emission energies.[25a] However, Casper and Meyer did not consider the participation of decay from the ^{3}LF excited state even though they used a [Re(bpy)(CO)$_3$(PR$_3$)]$^+$ complex. Now we know the "appropriate" rate constants for the nonradiative decay from ^{3}MLCT—i.e., the k_{d1} values (Table 3), which were calculated with consideration of the participation of ^{3}LF as described above—and the 0−0 band energy gaps E_{00}(^{3}MLCT), and these data are plotted in Figure 9 according to the energy gap law. The k_{d1} values obtained in our study for **1a**−**i** (open circles) show a much better linear relationship than those calculated without consideration of the participation of the ^{3}LF state (solid circles). The inset in Figure 9 shows all the data obtained in our study, i.e., the data not only for **1** but also for **3** and **4**. The line has a slope of -8.4 ± 0.6 eV^{-1} and an intercept of 33.6 ± 1.3, whereas the values reported by Casper and Meyer for the rhenium bpy tricarbonyl complexes are -11.76 eV^{-1} and 40.21, respectively.[25a]

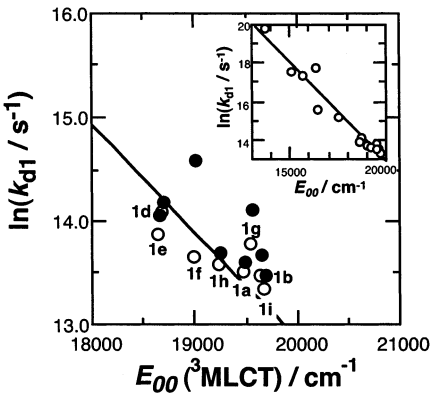

Figure 9. ln k_{d1} (○) and ln τ_e^{-1} (●) of **1a**−**i** vs E_{00}(^{3}MLCT) at 25 °C in a degassed CH$_3$CN solution. The inset depicts the same plots for **1**, **3**, and **4**.

Conclusion

The photochemical ligand substitution reactions of *fac*-[Re(X$_2$bpy)(CO)$_3$(PR$_3$)]$^+$ (**1**) proceed via a dissociation mechanism. The selective loss of the CO ligand from the position trans to the PR$_3$ ligand occurs from the ^{3}LF excited state. The thermodynamical data for the photochemical reactions of **1** have been obtained and are summarized in Table 3. In contrast to complexes **1**, complexes of the type *fac*-[Re(X$_2$bpy)(CO)$_2$(py)]$^+$ and *fac*-Re(X$_2$bpy)(CO)Cl were stable to 365 nm irradiation, and the temperature dependence of their emission lifetimes was considerably smaller than that for **1**. However, the ^{3}LF excited states of *fac*-[Re(bpy)(CO)$_3$(py)]$^+$ and *fac*-Re{(MeO)$_2$bpy}(CO)$_3$Cl at least are presumably accessible from the ^{3}MLCT states at ambient temperature. The photostabilities of these two complexes relative to **1** can be explained by the difference in the trans effects of the ligands PR$_3$, py, and Cl$^-$.

Acknowledgment. We thank Prof. Derk J. Stufkens (Universiteit van Amsterdam) and Prof. Yoko Kaizu (Tokyo Institute of Technology) for useful discussions and comments. This work was partially supported by Research and Innovative Technology for the Earth (RITE).

JA017032M

(46) The Re−C (of the axial CO) bond lengths measured by X-ray crystallographic analysis were 1.93 Å for **1a**[46a] and 1.88 Å for **3a**:[46b] (a) Ishitani, O.; Tsubaki, H.; Toyama, S. Unpublished result. (b) Lucia, L. A.; Abboud, K.; Schanze, K. S. *Inorg. Chem.* **1997**, *36*, 6224.